J|A|C|S
ARTICLES
Published on Web 11/30/2006

Steric Communication of Chiral Information Observed in Dendronized Polyacetylenes

Virgil Percec,*,† Emad Aqad,† Mihai Peterca,‡ Jonathan G. Rudick,† Lance Lemon,† Juan C. Ronda,† Binod B. De,† Paul A. Heiney,‡ and E. W. Meijer§

Contribution from the Roy & Diana Vagelos Laboratories, Department of Chemistry, University of Pennsylvania, Philadelphia, Pennsylvania 19104-6323, Department of Physics and Astronomy, University of Pennsylvania, Philadelphia, Pennsylvania 19104-6396, and Laboratory of Macromolecular and Organic Chemistry, Eindhoven University of Technology, P.O. Box 513, 5600 MB Eindhoven, The Netherlands

Received September 12, 2006; E-mail: percec@sas.upenn.edu

Abstract: Structural and retrostructural analysis of helical dendronized polyacetylenes (i.e., self-organizable polyacetylenes containing first generation dendrons or minidendrons as side groups) synthesized by the polymerization of minidendritic acetylenes with $[Rh(nbd)Cl]_2$ (nbd = 2,5-norbornadiene) reveals an ~10% change in the average column stratum thickness (*l*) of the cylindrical macromolecules with a chiral periphery, through which a strong preference for a single-handed screw-sense is communicated. The cylindrical macromolecules reversibly interconvert between a three-dimensional (3D) centered rectangular lattice ($\Phi_{r-c,k}$) exhibiting long-range intracolumnar helical order at lower temperatures and a two-dimensional (2D) hexagonal columnar lattice (Φ_h) with short-range helical order at higher temperatures. A polymer containing chiral, nonracemic peripheral alkyl tails is found to have a larger *l* as compared to the achiral polymers. In methyl cyclohexane solution, the same polymer exhibits an intense signal in circular dichroism (CD) spectra, whose intensity decreases upon heating. The observed change in *l* indicates that the chiral tails alter the polymer conformation from that of the corresponding polymer with achiral side chains. This change in conformation results in a relatively large free energy difference (ΔG_h) favoring one helix-sense over the other (per monomer residue). The capacity to distort the polymer conformation and corresponding free energy is related to the population of branches in the chiral tails and their distance from the polymer backbone by comparison to recently reported first and second generation dendronized polyphenylacetylenes.

Introduction

Helical chirality in macromolecules and supramolecular assemblies offers a wellspring of challenges and inspiration at the interface of scientific disciplines.[1−3] We, for example, have demonstrated the unique ability of dendritic dipeptide assemblies to form helical porous nanostructures inspired by transmembrane proteins.[4] We and others have identified helical arrangements of electroactive components as a critical opportunity to improve self-assembled organic electronics.[3,5,6] Chiral polymers that exhibit helical conformations are valued for molecular recognition and have been employed as stationary phase materials in HPLC columns and as sensory elements.[2,7]

Dynamic helical polymers exhibit an equilibrium between left- and right-handed screw-senses. The equilibrium can be shifted in the presence of chiral, nonracemic information either by appending the aromatic ring with chiral, nonracemic substituents or noncovalent association of chiral substrates.[1−3] The former approach is valuable in the chromatography[2a] and electronics examples above,[3,5,6] which require a static excess of single-handed chirality. The latter approach has been explored for sensor applications.[7] Principles for transfer of chiral information from side chains to the polymer backbone stress the importance of the chiral element-to-backbone distance and the need for steric or secondary bonding interactions to impede helix-sense reversal. Often, steric effects or hydrogen bonding are described in a fashion similar to the *i* to *i* + 3 connections

† Department of Chemistry, University of Pennsylvania.
‡ Department of Physics and Astronomy, University of Pennsylvania.
§ Eindhoven University of Technology.

(1) (a) Hill, D. J.; Mio, M. J.; Prince, R. B.; Hughes, T. S.; Moore, J. S. *Chem. Rev.* **2001**, *101*, 3893−4011. (b) Cornelissen, J. J. L.; Rowan, A. E.; Nolte, R. J. M.; Sommerdijk, N. A. J. M. *Chem. Rev.* **2001**, *101*, 4039−4070.
(2) (a) Nakano, T.; Okamoto, Y. *Chem. Rev.* **2001**, *101*, 4013−4038. (b) Tang, H. Z.; Tian, G.; Capracotta, M. D.; Novak, B. M. *J. Am. Chem. Soc.* **2004**, *126*, 3722.
(3) Hoeben, F. J. M.; Jonkheijm, P.; Meijer, E. W.; Schenning, A. P. H. J. *Chem. Rev.* **2005**, *105*, 1491−1546.
(4) Percec, V.; Dulcey, A. E.; Balagurusamy, V. S. K.; Miura, Y.; Smidrkal, J.; Peterca, M.; Nummelin, S.; Edlund, U.; Hudson, S. D.; Heiney, P. A.; Duan, H.; Magonov, S. N.; Vinogradov, S. A. *Nature* **2004**, *430*, 764−768.
(5) (a) Percec, V.; Glodde, M.; Bera, T. K.; Miura, Y.; Shiyanovskaya, I.; Singer, K. D.; Spiess, H.-W.; Hudson, S. D.; Duan, H. *Nature* **2002**, *417*, 384−387. (b) Percec, V.; Glodde, M.; Peterca, M.; Rapp, A.; Schnell, I.; Spiess, H.-W.; Bera, T. K.; Miura, Y.; Balagurusamy, V. S. K.; Aqad, E.; Heiney, P. A. *Chem.-Eur. J.* **2006**, *12*, 6298−6314.
(6) (a) Jonkheijm, P.; van der Schoot, P.; Schenning, A. P. H. J.; Meijer, E. W. *Science* **2006**, *313*, 80−83. (b) Percec, V.; Ungar, G.; Peterca, M. *Science* **2006**, *313*, 55−56.
(7) Yashima, E.; Maeda, K.; Nishimura, T. *Chem.-Eur. J.* **2004**, *10*, 42−51.
(8) (a) Yashima, E.; Huang, S.; Matsushima, T.; Okamoto, Y. *Macromolecules* **1995**, *28*, 4184−4193. (b) Nakako, H.; Mayahara, Y.; Nomura, R.; Tabata, M.; Masuda, T. *Macromolecules* **2000**, *33*, 3978−3982.

Scheme 1

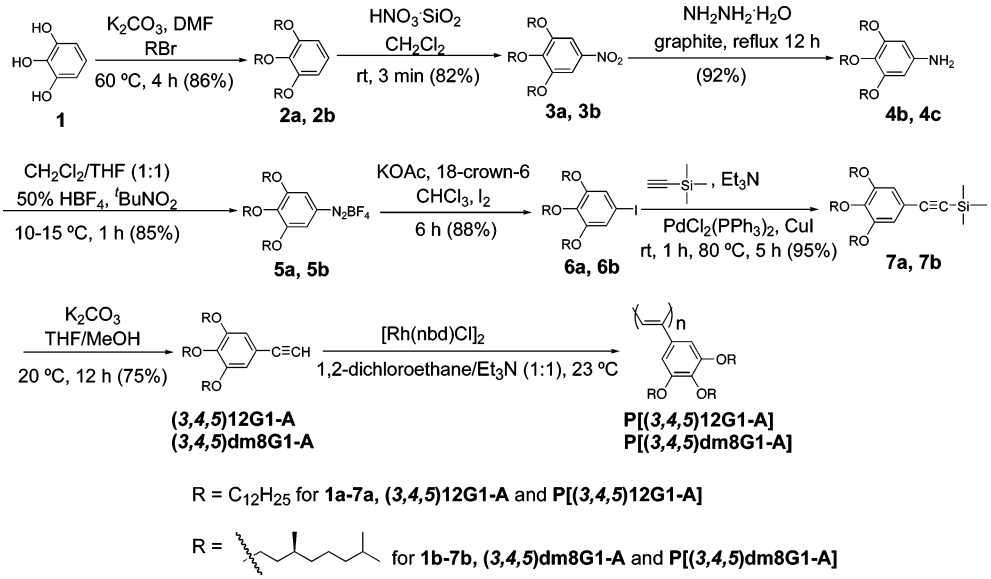

Scheme 2

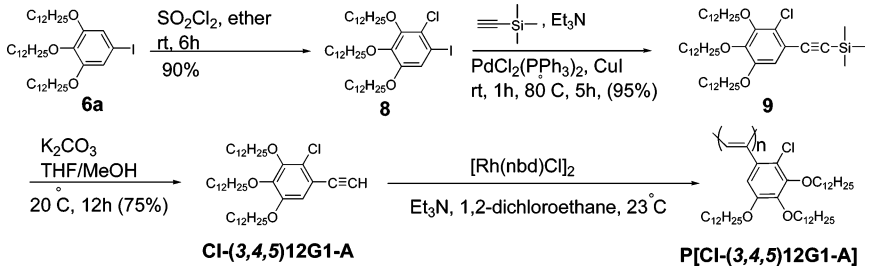

found in α-helical polypeptides.[8] *cis*-Polyarylacetylenes are dynamic helical polymers for which these rules have proven to be reliable.[2]

We have investigated helical chirality in dendronized polymers as a tool to program hierarchical ordering within self-organizable cylindrical and spherical macromolecules[9,10] and supramolecular assemblies.[11] 2-Ethynyl- and 3-ethynylcarbazole polymers carrying first generation self-assembling achiral and chiral dendrons (i.e., minidendrons) self-organize into nematic phases.[12] Interestingly, the copolymers of the chiral and achiral 2-ethynylcarbazole monomers exhibited a weaker sergeants-and-soldiers effect[13] than the corresponding 3-ethynylcarbazole copolymers even though the chiral, nonracemic 2-ethynylcarbazole homopolymer exhibits a larger circular dichroism (CD) signal associated with the helical polyene backbone than the 3-ethynylcarbazole homopolymer.[12] We have also reported a library of dendronized polyphenylacetylenes (PPAs) that exhibit hexagonal columnar lattices (Φ_h).[14] It was shown that for specific dendron substitution patterns the Φ_h exhibited intracolumnar helical order whose screw sense can be selected by chiral, nonracemic alkyl tails at the periphery. CD spectra of a second generation dendronized PPA confirmed helix-sense selection over a remarkable distance.[14a]

Meijer and co-workers have reported[15] structural analysis of **poly[(3,4,5)12G1-A]** (**P[(3,4,5)12G1-A**]) and **poly[(3,4,5)-dm8G1-A]** (**P[(3,4,5)dm8G1-A]**) (Scheme 1) and chiroptical properties of the latter in *ortho*-dichlorobenzene. These are polyacetylenes carrying self-assembling minidendrons. The XRD pattern from an unoriented **P[(*3,4,5*)12G1-A]** sample at 50 °C revealed a single low-angle diffraction peak, which was ascribed to an interdigitated lamellar liquid crystalline phase.

(9) (a) Percec, V.; Anh, C.-H.; Ungar, G.; Yeardley, D. J. P.; Möller, M.; Sheiko, S. S. *Nature* **1998**, *391*, 161−164. (b) Percec, V.; Anh, C.-H.; Barboiu, B. *J. Am. Chem. Soc.* **1997**, *119*, 12978−12979. (c) Percec, V.; Anh, C.-H.; Cho, W.-D.; Jamieson, A. M.; Kim, J.; Leman, T.; Schmidt, M.; Gerle, M.; Möller, M.; Prokhorova, S. A.; Sheiko, S. S.; Cheng, S. Z. D.; Zhang, A.; Ungar, G.; Yeardley, D. J. P. *J. Am. Chem. Soc.* **1998**, *120*, 8619−8631. (d) Percec, V.; Heck, J.; Tomazos, D.; Falkenberg, F.; Blackwell, H.; Ungar, G. *J. Chem. Soc. Perkin Trans. 1* **1993**, 2799−2811.

(10) Yeardley, D. J. P.; Ungar, G.; Percec, V.; Holerca, M. N.; Johansson, G. *J. Am. Chem. Soc.* **2000**, *122*, 1684−1689.

(11) (a) Hudson, S. D.; Jung, H.-T.; Percec, V.; Cho, W.-D.; Johansson, G.; Ungar, G.; Balagurusamy, V. S. K. *Science* **1997**, *278*, 449−452. (b) Ungar, G.; Liu, Y.; Zeng, X.; Percec, V.; Cho, W.-D. *Science* **2003**, *299*, 1208−1211. (c) Zeng, X.; Ungar, G.; Liu, Y.; Percec, V.; Dulcey, A. E.; Hobbs, J. K. *Nature* **2004**, *428*, 157−160. (d) Percec, V.; Cho, W.-D.; Ungar, G.; Yeardley, D. J. P. *J. Am. Chem. Soc.* **2001**, *123*, 1302−1315. (e) Percec, V.; Mitchell, C. M.; Cho, W.-D.; Uchida, S.; Glodde, M.; Ungar, G.; Zeng, X.; Liu, Y.; Balagurusamy, V. S. K.; Heiney, P. A. *J. Am. Chem. Soc.* **2004**, *126*, 6078−6094. (f) Percec, V.; Peterca, M.; Sienkowska, M. J.; Ilies, M. A.; Aqad, E.; Smidrkal, J.; Heiney, P. A. *J. Am. Chem. Soc.* **2006**, *128*, 3324−3334. (g) Percec, V.; Holerca, M. N.; Nummelin, S.; Morrison, J. J.; Glodde, M.; Smidrkal, J.; Peterca, M.; Rosen, B. M.; Uchida, S.; Balagurusamy, V. S. K.; Sienkowska, M. J.; Heiney, P. A. *Chem.-Eur. J.* **2006**, *12*, 6216−6241. (h) Li, Y.; Lin, S.-T.; Goddard, W. A. III. *J. Am. Chem. Soc.* **2004**, *126*, 1872−1885.

(12) Percec, V.; Obata, M.; Rudick, J. G.; De, B. B.; Glodde, M.; Bera, T. K.; Magonov, S. N.; Balagurusamy, V. S. K.; Heiney, P. A. *J. Polym. Sci. Part A: Polym. Chem.* **2002**, *40*, 3509−3533.

(13) (a) Green, M. M.; Reidy, M. P.; Johnson, R. J.; Darling, G.; O'Leary, D. J.; Wilson, G. *J. Am. Chem. Soc.* **1989**, *111*, 6452−6454. (b) Green, M. M.; Peterson, N. C.; Sato, T.; Teramoto, A.; Cook, R.; Lifson, S. *Science* **1995**, *268*, 1860−1866. (c) Green, M. M.; Cheon, K.-S.; Yang, S.-Y.; Park, J.-W.; Swansburg, S.; Liu, W. *Acc. Chem. Res.* **2001**, *34*, 672−680.

(14) (a) Percec, V.; Rudick, J. G.; Peterca, M.; Wagner, M.; Obata, M.; Mitchell, C. M.; Cho, W.-D.; Balagurusamy, V. S. K.; Heiney, P. A. *J. Am. Chem. Soc.* **2005**, *127*, 15257−15264. (b) Percec, V.; et al. *Chem.-Eur. J.* **2006**, *12*, 5731−5746.

(15) Schenning, A. P. H. J.; Fransen, M.; Meijer, E. W. *Macromol. Rapid Commun.* **2002**, *23*, 265−270.

Table 1. Polymerization Conditions and Structural Characteristics of the Polymers[a]

polymer	$[M]_0$ (M)	$[M]_0/[Rh]_0$	reaction time (h)	yield (%)	$M_n \times 10^{-3}$ [b]	M_w/M_n [b]	*cis*-content (%)[c]
P[(*3,4,5*)12G-A]	0.072	179	14	84	188	1.21	91
P[(*3,4,5*)dm8G1-A]	0.081	87	12	80	71	1.42	89
P[Cl-(*3,4,5*)12G1−A]	0.066	50	12	65	29	1.57	85

[a] Polymerizations were carried out with $[Rh(nbd)Cl]_2$ in 1,2-dichloroethane/NEt_3 (10:1 v/v) at 23 °C. [b] Determined by GPC (THF, 1 mL × min^{-1}) calibrated with polystyrene standards. [c] Determined as described in ref 21a.

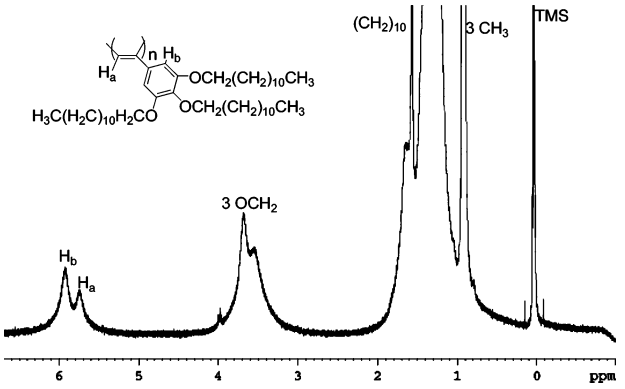

Figure 1. ^1H NMR Spectrum of **P[(*3,4,5*)12G1-A]** in $CDCl_3$.

Variable-temperature CD spectra of **P[(*3,4,5*)dm8G1-A]** demonstrated that the polymer backbone exhibits a helical conformation whose handedness reversibly inverts upon heating (i.e., stereomutation). Percec and co-workers have previously investigated bulk self-assembly and self-organization of **P[(*3,4,5*)-12G1-A]** and its analogue **poly[Cl-(*3,4,5*)12G1-A]** (**P[(*3,4,5*)-12G1-A]**) (Scheme 2). However, the results of these experiments were not published.[16] We have re-synthesized and re-investigated these structures[15,16] to elucidate structural parameters for communicating chiral information over increasingly larger distances.

Herein we report the synthesis of three minidendritic acetylene monomers and their polymerization using [Rh(nbd)Cl]2 (nbd = 2,5−norbornadiene).[17] First generation self-assembling dendrons, or minidendrons, serve as models for the elaboration and elucidation of novel self-assembly processes found in larger dendrons.[18,10,19] This is analogous to simple peptide sequences used to understand molecular engineering principles for assembling more complex protein structures.[20] In methyl cyclohexane solution, we confirm using CD spectroscopy that **P[(3,4,5)dm8G1-A]** adopts a preferred helix screw-sense and that this preference decreases with increasing temperature. The corresponding UV−vis spectra indicate stretching of the polyene backbone as evidenced by a red shift of the long wavelength absorption. XRD studies of the polymers in bulk and in oriented fibers revealed additional low-angle diffraction peaks. The

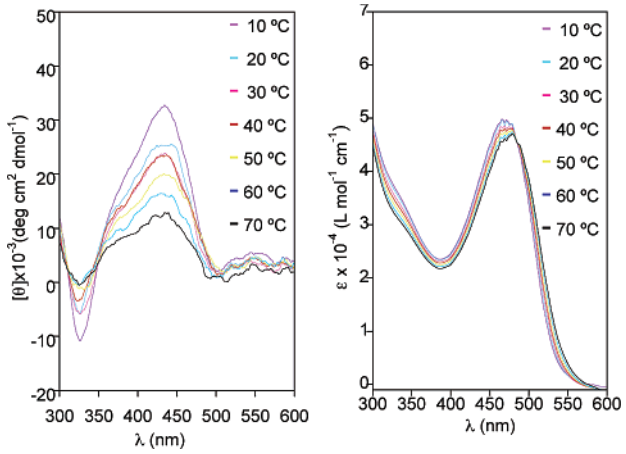

Figure 2. Variable-temperature CD (left side) and UV−vis (right side) spectra of **P[(*3,4,5*)dm8G1-A]** (2.4×10^{-4} M) in methyl cyclohexane.

Table 2. Thermal Transitions and Corresponding Enthalpy Changes of the Self-Organized Periodic Arrays of Dendronized Polyacetylenes

polymer	thermal transitions (°C) and corresponding enthalpy changes (kcal/mol)[a]: first and second heating scans (°C, kcal/mol)	first cooling scan (°C, kcal/mol)
P [(*3,4,5*)12G1-A]	$\Phi_{r-c,k}$[b] 46 (4.20) Φ_h[c] $\Phi_{r-c,k}$ 24 (2.85) Φ_h	Φ_h 21 (3.60) $\Phi_{r-c,k}$
P [(*3,4,5*)dm8G1-A]	$\Phi_{r-c,k}$ 14 (0.38) Φ_h $\Phi_{r-c,k}$ 15 (0.41) Φ_h	Φ_h−15 (0.27) $\Phi_{r-c,k}$
P[Cl-(*3,4,5*)12G1-A]	$\Phi_{r-c,k}$ 36 (3.41) Φ_h $\Phi_{r-c,k}$ 35 (3.74) Φ_h	Φ_h 24 (3.40) $\Phi_{r-c,k}$

[a] Thermal transitions (°C) and enthalpy changes in between parenthesis (kcal/mol) were determined by DSC (10 °C/min). Data from the first heating and cooling scans are on the first line, and data from the second heating scans are on the second line. [b] $\Phi_{r-c,k}$ = *c2mm* 3D centered rectangular columnar lattice. [c] Φ_h = *p6mm* 2D columnar hexagonal lattice.

cylindrical macromolecules reversibly interconvert between a three-dimensional (3D) centered rectangular lattice ($\Phi_{r-c,k}$) at lower temperatures and a two-dimensional (2D) Φ_h lattice at higher temperatures. Intracolumnar helical order is found in both phases for all polymers. **P[(3,4,5)dm8G1-A]** has a larger average column stratum thickness (*l*) as compared to **P[(3,4,5)-12G1-A]** and **P[Cl-(3,4,5)12G1-A]**. For the first time, the steric effect involved in communication of chiral information to the polymer backbone is shown to result in distortion of the helical conformation relative to an achiral congener. The magnitude of the distortion relates to the magnitude of the free energy difference (ΔG_h) favoring one helix-sense over the other.

Results and Discussion

Synthesis of Dendritic Acetylenes. Dendritic monomers were prepared as described in Schemes 1 and 2 by a new synthetic method.[15] This method allows the synthesis of the previously unknown ortho-substituted compounds from Scheme 2. Details are described in Supporting Information.

(16) Lemon, L. Synthesis and polymerization of arylacetylene monomers. M.S. Thesis, Case Western Reserve University, Cleveland, OH, 1996.
(17) Sedlácek, J.; Vohlídal, J. *Collect. Czech. Chem. Commun.* **2003**, *68*, 1745−1790.
(18) Percec, V.; Anh, C.-H.; Bera, T. K.; Ungar, G.; Yeardley, D. J. P. *Chem.-Eur. J.* **1999**, *5*, 1070−1083.
(19) (a) Percec, V.; Holerca, M. N.; Magonov, S. N.; Yeardley, D. J. P.; Ungar, G.; Duan, H.; Hudson, S. D. *Biomacromolecules* **2001**, *2*, 706−728. (b) Percec, V.; Holerca, M. N.; Uchida, S.; Yeardley, D. J. P.; Ungar, G. *Biomacromolecules* **2001**, *2*, 729−740. (c) Duan, H.; Hudson, S. D.; Ungar, G.; Holerca, M. N.; Percec, V. *Chem.-Eur. J.* **2001**, *7*, 4134−4141. (d) Percec, V.; Holerca, M. N.; Uchida, S.; Cho, W.-D.; Ungar, G.; Lee, Y.; Yeardley, D. J. P. *Chem.-Eur. J.* **2002**, *8*, 1106−1117.
(20) Robertson, D. E.; Farid, R. S.; Moser, C. S.; Urbauer, J. L.; Mugholland, S. E.; Podikiti, R.; Lear, J. D.; DeGrado, W. F.; Dutton, P. L. *Nature* **1994**, *368*, 425−432.

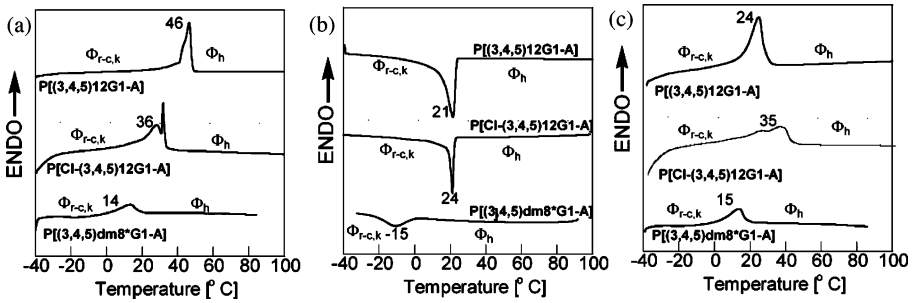

Figure 3. DSC traces of **P[(*3,4,5*)12G1-A]**, **P[Cl-(*3,4,5*)12G1-A]**, and **P[(*3,4,5*)dm8G1-A]**: (a) first heating; (b) first cooling; (c) second heating.

Table 3. Measured *d*-Spacings and Structural Analysis of the Self-Organized Periodic Arrays of Dendronized Polyacetylenes

polymer	*T* (°C)	lattice	*d*-Spacings (Å)	*a* or *(a, b)* (Å)	D_{col} (Å)
P[(*3,4,5*)12G1-A]	80	Φ_h	d_{10} (23.3) d_{11} (13.4)	26.90[a]	26.90[c]
	40	$\Phi_{r-c,k}$	d_{20} (24.6) d_{11} (20.2)	49.27, 22.09[b]	31.4,[d] 22.09[e]
P[(*3,4,5*)dm8G1-A]	80	Φ_h	d_{10} (21.3)	24.32	24.32
	24	Φ_h	d_{10} (21.1)	24.6	24.6
	−40	$\Phi_{r-c,k}$	d_{20} (21.9) d_{11} (19.0)	43.83, 21.13	27.9, 21.13
P[Cl-(*3,4,5*)12G1-A]	60	Φ_h	d_{10} (23.5) d_{11} (13.5)	27.09	27.09
	24	$\Phi_{r-c,k}$	d_{20} (25.0) d_{11} (20.3)	49.90, 22.20	31.8, 22.2

[a] *p6mm* = 2D hexagonal columnar (Φ_h); $a = 2\langle d_{100}\rangle\sqrt{3}$, $\langle d_{100}\rangle = (d_{100} + \sqrt{3}d_{110})/2$. [b] *c2mm* = 3D centered rectangular ($\Phi_{r-c,k}$) lattice parameters *a* and *b*; $a = h0$, $b = k0$; ($h0$) and ($k0$) from diffractions. [c] Column diameter for the Φ_h phase, $D_{col} = a$. [d] Column diameter along the *a*-direction of the $\Phi_{r-c,k}$ phase, $D_{col} = 2a/\pi$. [e] Column diameter along the *b*-direction of the $\Phi_{r-c,k}$ phase, $D_{col} = b$.

Polymerization of Monomers and Characterization of the Polymers in Solution. All monomers were polymerized using $[Rh(nbd)Cl]_2$ at 23 °C in 1,2-dichloroethane/NEt_3 (10:1 v/v). Table 1 reports the reaction conditions, the number (M_n) and weight (M_w) average molecular weights, and the stereochemistry of the polymers. Figure 1 depicts the ^{1}H NMR spectrum of **P-[(3,4,5)12G1-A]** in $CDCl_3$. The *cis*-polyene proton is visible at ~5.7 ppm.[21] The cis-content of all polymers was determined from ^{1}H NMR spectra using a method developed in our group.[21]

Typically we would also be concerned with the formation of intramolecular 1,3-cyclohexadiene sequences along the polymer backbone via electrocyclization.[14,21−25] However, the alkoxy methylene overlaps the methine resonance of the cyclohexadiene units so that we cannot assess these defects.[14] Nevertheless, the high cis-content indicates that 1,3-cyclohexadiene defects cannot be significant in these dendronized polymers. Additionally, we have shown that their occurrence is usually negligible even for PPA prepared with Rh(I)-based catalysts.[22]

Figure 2 presents variable-temperature CD and UV−vis spectra of **P[(3,4,5)dm8G1-A]** in methyl cyclohexane. The long wavelength absorption in the UV−vis spectrum is associated with conjugation along the polyene backbone; therefore, the signal in this region of the CD spectrum indicates that the polyene backbone adopts a preferred helical screw sense. Upon heating from 10 to 70 °C, the intensity of the CD signal decreases, and a red shift in the UV−vis spectrum is observed.[2,7,8,12−14a,15,23,26] In contrast to our observations with poly[4-((+)-l-mentholoxycarbonyl)phenylacetylene],[23] subsequent cooling and heating show no hysteresis. Therefore, for the time scale of the experiment, intramolecular electrocyclization of the PPA backbone is not significant.

Structural and Retrostructural Analysis of the Dendronized Polymers. Thermal optical polarized microscopy (TOPM) and differential scanning calorimetry (DSC) were used to identify transition temperatures. Figure 3 depicts DSC traces of all polymers. Reversible heating and cooling cycles are observed. Samples from DSC experiments were analyzed by GPC to confirm the thermal stability of the polymers. Table 2 enumerates the transition temperatures and corresponding enthalpy changes. The large enthalpies and supercooling are consistent with the 3D order of the low-temperature phase. Branching in the peripheral alkyl chains results in a depression of the melting temperature and lower transition enthalpy. Furthermore, during the second DSC heating scans **P[Cl-(*3,4,5*)-12G1-A]** has slightly higher temperature transitions than **P-[(*3,4,5*)12G1-A]**. This might be a consequence of the dipole introduced by the chlorine.

The columnar phases identified by DSC and TOPM were assigned by XRD. Table 3 reports the lattice symmetry, observed *d*-spacings, lattice parameter (*a* and *b* for the $\Phi_{r-c,k}$ phase and *a* for the Φ_h phase), and column diameter (D_{col}) of each phase. Notably, we have indexed both d_{20} and d_{11} reflections in the $\Phi_{r-c,k}$ phase for all three polymers. For **P[(*3,4,5*)12G1-A]** and **P[Cl-(*3,4,5*)12G1-A]**, we have indexed both the d_{10} and d_{11} reflections in the Φ_h phase. All three polymers exhibit a $\Phi_{r-c,k}$ phase at low temperature and a Φ_h phase at higher temperature. This clearly eliminates the previous lamellar phase assignment for **P[(*3,4,5*)12G1-A]** at 50 °C.[15] Despite the differences in

(21) (a) Simionescu, C. I.; Percec, V.; Dumitrescu, S. *J. Polym. Sci. Polym. Chem. Ed.* **1977**, *15*, 2497−2509. (b) Simionescu, C. I.; Percec, V. *J. Polym. Sci. Polym. Lett. Ed.* **1979**, *17*, 421−429. (c) Simionescu, C. I.; Percec, V. *J. Polym. Sci. Polym. Chem. Ed.* **1980**, *18*, 147−155.
(22) Percec, V.; Rudick, J. G. *Macromolecules* **2005**, *38*, 7241−7250.
(23) Percec, V.; Rudick, J. G.; Aqad, E. *Macromolecules* **2005**, *38*, 7205−7206.
(24) (a) Percec, V.; Rudick, J. G.; Nombel, P.; Buchowicz, W. *J. Polym. Sci. Part A: Polym. Chem.* **2002**, *40*, 3212−3220. (b) Percec, V.; Rinaldi, P. L. *Polym. Bull.* **1983**, *9*, 548−555. (c) Percec, V. *Polym. Bull.* **1983**, *10*, 1−7.
(25) (a) Kishimoto, Y.; Eckerle, P.; Miyatake, T.; Ikariya, T.; Noyori, R. *J. Am. Chem. Soc.* **1994**, *116*, 12131−12132. (b) Kishimoto, Y.; Eckerle, P.; Miyatake, T.; Kainosho, M.; Ono, A.; Ikariya, T.; Noyori, R. *J. Am. Chem. Soc.* **1999**, *121*, 12035−12044.
(26) (a) Morino, K.; Maeda, K.; Okamoto, Y.; Yashima, E.; Sato, T. *Chem.-Eur. J.* **2002**, *8*, 5112−5120. (b) Hasegawa, T.; Morino, K.; Tanaka, Y.; Katagiri, H.; Furusho, Y.; Yashima, E. *Macromolecules* **2006**, *39*, 482−488. (c) Nomura, R.; Fukushima, Y.; Nakako, H.; Masuda, T. *J. Am. Chem. Soc.* **2000**, *122*, 8830−8836.

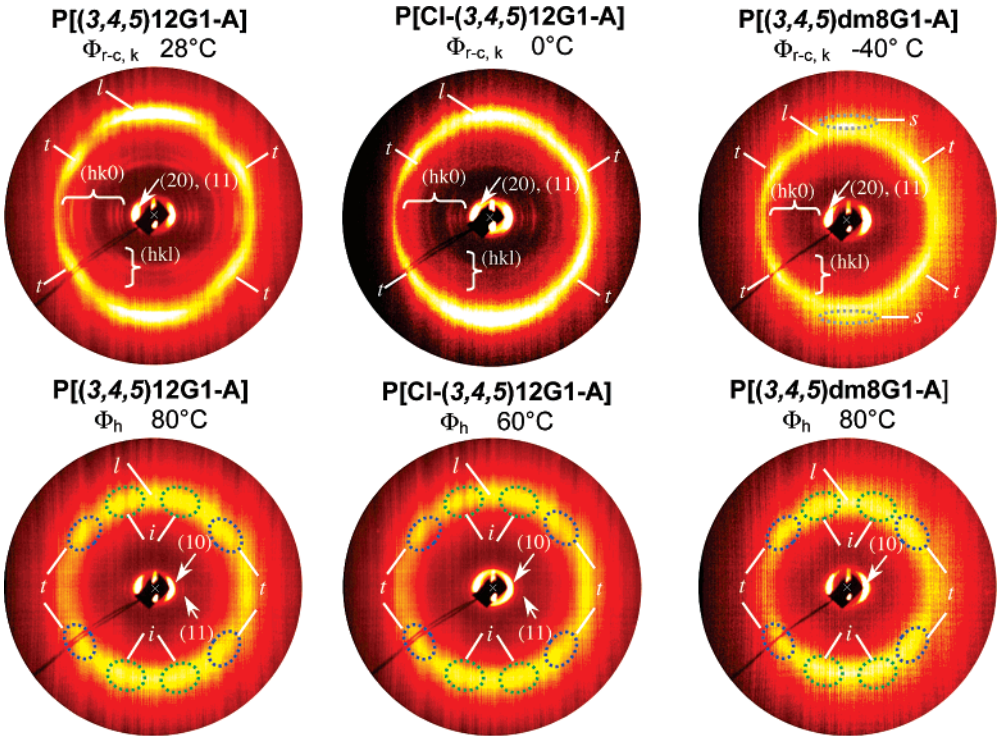

Figure 4. Wide-angle X-ray diffraction patterns of aligned fibers collected at the indicated temperatures; the fiber axis is vertical. *l*, average column stratum thickness; *i*, diffuse short-range helical feature; *t*, dendron tilt feature; *s*, 4.3 Å stacking along the column feature; (10), (11), (*hk*0) reflections of the 2D Φ_h phase; (*hkl*) and (*hk*0), (*hkl*) reflections of the 3D $\Phi_{r-c,k}$ phase.

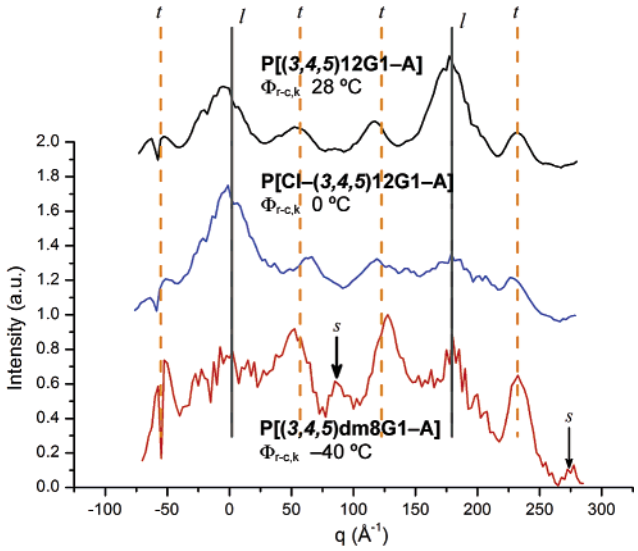

Figure 5. Azimuthal angle χ plots for the fiber patterns shown in Figure 4.

molecular structure, there is very little difference in D_{col} found in the Φ_h phase for each polymer. In the Φ_h phase the lattice parameter, *a*, is equivalent to the diameter of the cylindrical macromolecule (D_{col}).

XRD patterns from oriented fibers of each polymer in its $\Phi_{r-c,k}$ and Φ_h phase are presented in Figure 4. In the $\Phi_{r-c,k}$ phase, no significant differences of the dendron tilt feature (*t* in Figures 4 and 5) or of the position of the first-order (*hk*) reflections between polymers were observed. The only major difference is the larger value of the average column thickness (*l* in Figures 4 and 5) of the chiral polymer. This trend is observed in both the Φ_h and the $\Phi_{r-c,k}$ phases. For **P[(*3,4,5*)-dm8G1-A]** *l* is 4.5 and 4.8 Å in the $\Phi_{r-c,k}$ and Φ_h phases, respectively, whereas *l* for the achiral polymers is 4.1 and 4.4 Å in the $\Phi_{r-c,k}$ and Φ_h phases, respectively (Figure 6). A larger (i.e., 7.5 Å vs 7.2 Å) first-order (*hk*) reflection position (i.e., 7.5 Å vs 7.2 Å) for **P[(*3,4,5*)dm8G1-A]** is shown in the meridional *q*-plots (Figure 6a).

P[(*3,4,5*)12G1-A], **P[(*3,4,5*)dm8G1-A]**, and **P[Cl-(*3,4,5*)-12G1-A]** are high *cis*-content stereoregular *cis*-transoidal dendronized polyacetylenes that in bulk behave as cylindrical objects that self-organize into 3D $\Phi_{r-c,k}$ and 2D Φ_h phases. From the structural information presented above, we have prepared a model that describes the intracolumnar organization of **P[(*3,4,5*)12G1-A]** (Figure 7). The helical arrangement enforced by the polyene backbone and the dendritic side groups is highlighted. The dihedral angle (θ) is set to account for the observed structural features.

The model in Figure 7 is general for the three dendronized polyacetylenes. In the low temperature $\Phi_{r-c,k}$ phase common to the three polymers, we do not find significant differences in the dendron tilt feature (*t* in Figures 4 and 5) or the first-order (*hk*) reflection position. Both observations suggest that the polymers adopt similar 3D arrangements in the $\Phi_{r-c,k}$ phase. Comparing the column diameter of **P[(*3,4,5*)12G1-A]**, **P[(*3,4,5*)-dm8G1-A]**, and **P[Cl-(*3,4,5*)12G1-A]** in the 2D Φ_h phase (Table 3) also points to structures that are very similar to each other.

Both the DSC and XRD results indicate that the transition from the 3D $\Phi_{r-c,k}$ to 2D Φ_h phase is largely related to packing of the peripheral alkyl tails. Dramatic decreases in the melt transition temperature and transition enthalpy are found for **P-[(*3,4,5*)dm8G1-A]** as compared to **P[(*3,4,5*)12G1-A]** and **P-[Cl-(*3,4,5*)12G1-A]** (Table 2, Figure 3). Branching in the chiral tails is the likely source of these differences. Furthermore, the small variations of D_{col} and *l* with temperature observed by XRD

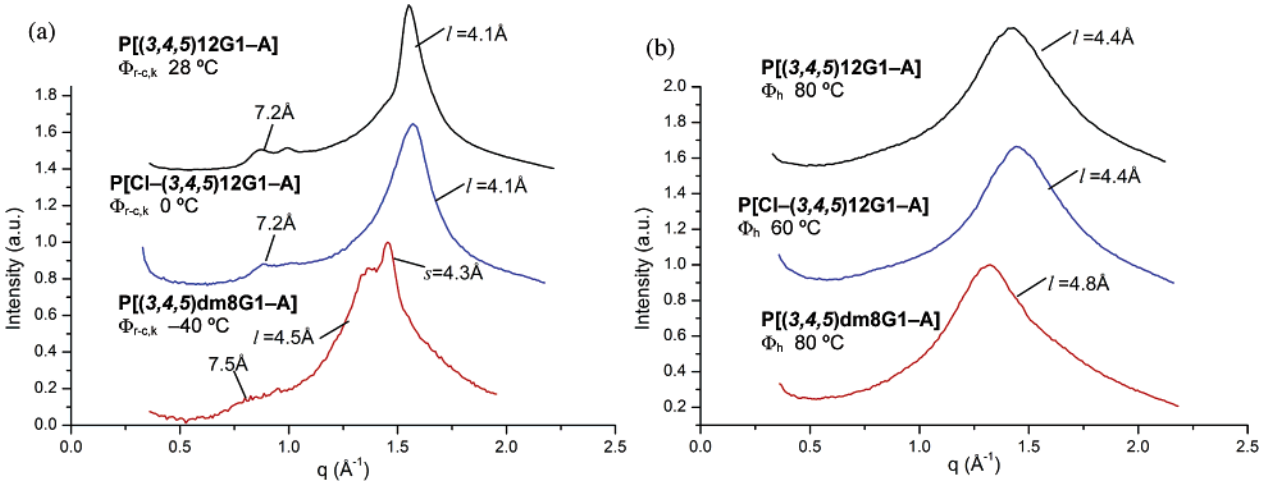

Figure 6. Meridional *q* plots for the fiber patterns shown in Figure 4 for the 3D $\Phi_{r-c,k}$ phase (a) and for the 2D Φ_h phase (b).

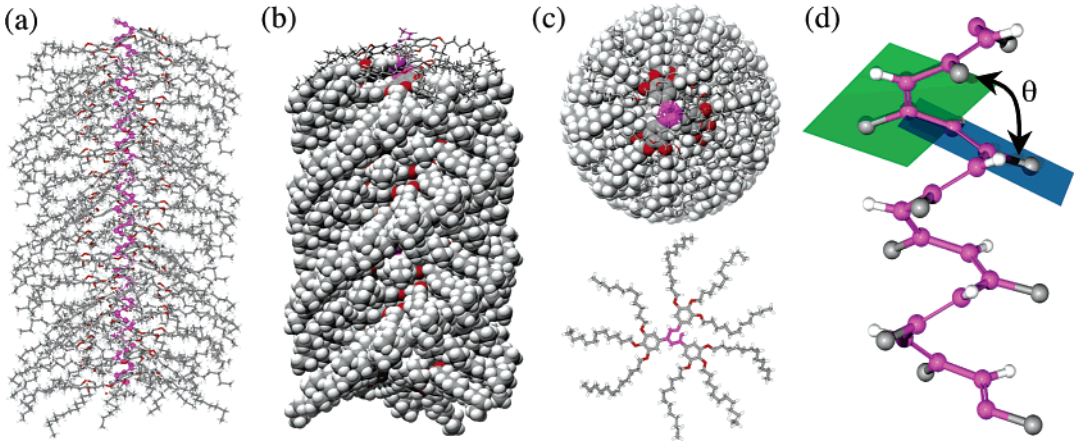

Figure 7. Structure of the cylindrical **P[(*3,4,5*)12G1-A]**. Side-view renderings as (a) stick and (b) space filling models, (c) top view of the column and of a column stratum, and (d) detail of the polymer backbone. An increase of the indicated dihedral angle (θ) of approximately 3−5° is enough to modify the average column stratum thickness from 4.1 Å observed in the 3D $\Phi_{r-c,k}$ phase to 4.4 Å in the 2D Φ_h phase.

indicate that also small changes in the backbone conformation take place during the $\Phi_{r-c,k}$ to Φ_h phase transition. It is most likely that the major changes that the columns undergo during this transition are in the alkyl tails. In the low temperature $\Phi_{r-c,k}$ phase, the rigidity of the tails distorts space-filling at the periphery of the column. At higher temperatures, in the Φ_h phase, increased flexibility allows the formation of the Φ_h organization.

Similar to other polyarylacetylenes these dendronized polymers are dynamic helical polymers. Helical order has been identified in both the $\Phi_{r-c,k}$ and Φ_h phases of **P[(*3,4,5*)dm8G1-A]**. From CD spectra in methyl cyclohexane, we recognize that the chiral alkyl chains in **P[(*3,4,5*)dm8G1-A]** are able to select a preferred screw-sense for the helical backbone. The screw-sense bias is temperature-dependent.[26] Helical order has also been identified in both the $\Phi_{r-c,k}$ and Φ_h phases of the two polymers derived from achiral monomers. On the basis of the close structural analogy between the three polymers, we can gain insight to the mechanism by which helix-sense selection occurs.

According to the model for macromolecular helix-sense selection developed by Green and co-workers,[13] both helical-senses will be found in polymers with achiral side chains if the degree of polymerization is greater than the persistence length of a helical segment. This is because there is no free energy difference to favor one helix sense or the other per monomer residue ($\Delta G_h = 0$, Scheme 3). Separating the oppositely handed helical segments is a helix reversal with which there is an associated excess energy (ΔG_r). On the other hand, in a polymer with chiral, nonracemic monomers there is preferred helix-sense because there is a free energy penalty for putting the monomer in its non-preferred helical conformation. Scheme 3 illustrates two scenarios for a helical polymer with chiral, nonracemic side

Scheme 3[a]

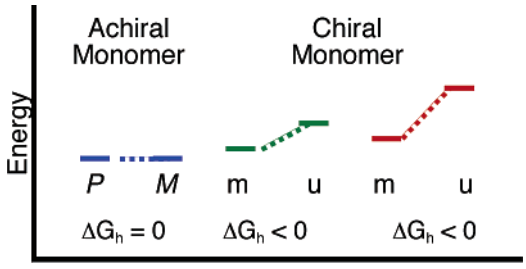

[a] For the achiral monomer scenario, *P* and *M* refer to the respective helix screw sense. For the chiral monomer scenarios, the matched (m) and unmatched (u) energy levels correspond to the monomer in its preferred and non-preferred helical screw senses, respectively.

chains. In one case, the polymer with chiral side chains adopts a conformation very similar to the achiral polymer. The chiral information in the side chain creates a modest ΔG_h, which translates into weak helix-sense selection. In the second scenario, the polymer with chiral side chains adopts a conformation more different from the achiral polymer. A larger ΔG_h manifests greater bias of a single preferred helix-sense.

From XRD of oriented fiber samples we have seen that the average column stratum thickness (*l*) is significantly larger for **P[(*3,4,5*)dm8G1-A]** than **P[(*3,4,5*)12G1-A]** or **P[Cl-(*3,4,5*)-12G1-A]** in both the $\Phi_{r-c,k}$ and Φ_h phases. Clearly, this larger layer separation is caused by the presence of methyl branches in the peripheral alkyl chains, including that of the chiral *C*(3). Evidence that this increase is transmitted to the core region can be seen in the larger *d*-spacings of the first order (*hk*) reflection in the $\Phi_{r-c,k}$ phase. Our model shows that a small change in dihedral angle (θ) can accommodate the necessary structural changes (Figure 7d).

Recently we have reported a library of dendronized PPAs.[14] Some of the polymers contain chiral alkyl tails at the periphery. For the second generation dendronized PPA, **poly[(*3,4*−*3,5*)*m*G2−4EBn]**, with achiral (m = 12) and chiral (m = dm8) alkyl chains there is no significant change in *l* (4.1 Å). In methyl cyclohexane solution, **poly[(*3,4*−*3,5*)dm8G2−4EBn]** exhibits a signal in the polyene backbone region of the CD spectrum at 2 °C that decreases upon warming to 22 °C. We associate this behavior with the chiral information in the peripheral alkyl tails being less efficiently conveyed to the polymer backbone in the second generation PPAs as compared to dendronized polyacetylenes herein.

Greater bias in the helix-sense selection by **P[(*3,4,5*)dm8G1-A]** than **poly[(*3,4*−*3,5*)dm8G2−4EBn]** is a consequence of a larger energy penalty (ΔG_h) for placing the chiral monomer into its non-preferred helix-sense. The behavior observed for **P-[(*3,4,5*)12G1-A]** and **poly[(*3,4*−*3,5*)12G2−4EBn]** is illustrated by the "achiral monomer" scenario in Scheme 3. We liken the observed helix-sense selection by **poly[(*3,4*−*3,5*)dm8G2−4EBn]** to the middle energy diagram in Scheme 3. There is a negligible energy difference between the preferred helical handedness and the helix adopted by the polymer composed of achiral monomers. The penalty for putting the chiral, nonracemic monomer in its non-preferred helix-sense is correspondingly small. The final energy diagram in Scheme 3 is used to understand **P[(*3,4,5*)dm8G1-A]**, where we can find structural evidence for a conformational difference imposed by the chiral alkyl tails. The helical conformation adopted by **P[(*3,4,5*)-dm8G1-A]** has a distinctly different energy than that adopted by **P[(*3,4,5*)12G1-A]**. The greater difference between the achiral and chiral polymers translates into a correspondingly larger energy penalty for placing the chiral monomer into its non-preferred helix-sense.

Drawing comparisons between the polymers herein and those of the previous library[14] indicate that the number of chiral, nonracemic centers should increase as their distance from the polymer backbone increases. First generation **poly[(*4*−*3,4,5*)*m*G1−4EBn]** is of comparable size to **poly[(*3,4*−*3,5*)*m*G2−4EBn]** for the same *m*. For example, when m = 12, the column diameter is 46.2 Å (115 °C) for **poly[(*4*−*3,4,5*)12G1−4EBn]**, and it is 44.9 Å (105 °C) for **poly[(*3,4*−*3,5*)12G2−4EBn]** in the Φ_h phase.[14] The former dendron carries three alkyl tails while the latter carries four. When the dodecyl chains are replaced with chiral, nonracemic alkyl tails the result is dramatically different. **Poly[(*4*−*3,4,5*)AmylG1−4EBn]** has chiral tails derived from (*S*)-amyl alcohol[27] but no signal is observed in the CD spectrum in methyl cyclohexane even at 2 °C. The distance of the chiral information from the polymer backbone is most clearly noticed by comparing the diameter of the cylindrical macromolecules in the Φ_h phase. **P[(*3,4,5*)-dm8G1-A]** has a column diameter of 24.6 Å (24 °C) while **poly-[(*3,4*−*3,5*)dm8G2−4EBn]** has a column diameter of 43 Å (23 °C).[14a] The lower melt temperature and transition enthalpy for **P[(*3,4,5*)dm8G1-A]** as compared to **P[(*3,4,5*)12G1-A]** dissuade us from the rationale that the dependence on the distance and population of chiral, nonracemic braches is to foster i to $i + n$ contacts that reinforce the preferred helical screw-sense.

We understand these structural effects by considering space-filling lateral to the dendron wedge (i.e., perpendicular to the column). The chiral carbons are relatively confined to fit along the circumference of a circle of given diameter, which is determined by the size of the dendron or distance to the cylinder core. As the population of chiral carbons increases without changing the diameter, the chiral centers begin to get crowded. A critical level of crowding appears necessary to achieve even small degrees of helix-sense selection. When overcrowding occurs, the vertical dimension of the dendron (i.e., parallel to the cylinder axis) must compensate. The increase of the average column stratum thickness (*l*), as observed here experimentally, is the product of overcrowding.

Conclusions

Structural and retrostructural analysis of three dendronized polyacetylenes has shed light on the molecular mechanism by which chiral information is conveyed over large distances in dynamically helical polyacetylenes. Steric effects due to branching in the side chain can distort the polymer backbone conformation compared to one without branching. When this steric bulk is associated with a chiral center, the change in conformation distorts the free energy difference (ΔG_h) favoring one helix-sense over the other (per monomer residue). The magnitude of such distortions is related to the population of chiral branches and their distance from the polymer backbone. Peripheral chiral, nonracemic alkyl tails in dendronized polymers are able to impose a conformational change that stretches the polymer backbone. We have observed this directly as the ~10% increase of the average column stratum thickness (*l*) in XRD patterns of oriented fibers of **P[(3,4,5)dm8G1-A]** as compared to **P[(3,4,5)12G1-A]** and **P[Cl-(3,4,5)12G1-A]**. CD spectra of **P[(3,4,5)dm8G1-A]** in methyl cyclohexane confirm that the polymer backbone adopts a preferred helix-sense. This is the first example where the steric impact of chiral branching has been shown to directly relate to communication of chiral information. The model described above contrasts with other explanations[2,7,8,26] for steric communication of chiral information in that it does not require chiral groups to associate like teeth

(27) Helix sense−selection was possible for dendronized poly(ethynylcarbazole)s with (*S*)-amyl tails; see ref 9.

(28) For recent selected reviews and highlights on dendronized polymers, see: (a) Percec, V. *Phil. Trans. R. Soc. A* **2006**, *364*, 2709−2719. (b) Schlüter, A. D. *Top. Curr. Chem.* **2005**, *245*, 151−191. (c) Frauenrath, H. *Prog. Polym. Sci.* **2005**, *30*, 325−384.

in a set of gears, nor does it invoke atropisomeric conformations between the conjugated polymer backbone and the aromatic side chain. The potential generality of this mechanism in other related macromolecular and supramolecular helical structures is under investigation. The experiments reported here also support the hypothesis that the higher dynamics of minidendrons allows them to be used as models or maquettes[18,20] that can assess the molecular mechanism of structure formation[19] in higher generations of self-organizable dendronized polymers.[14,28]

Acknowledgment. Financial support by the National Science Foundation (DMR-0548559 and DMR-0520020) and P. Roy Vagelos Chair at Penn are gratefully acknowledged.

Supporting Information Available: Experimental section containing materials, techniques, synthesis, and analytical data; a discussion of the monomer synthesis; a discussion of the chiral, nonracemic monomers; the complete ref 14b. This material is available free of charge via the Internet at http://pubs.acs.org.

JA0665848